

## ABSTRACT

Lysophosphatidic acid (LPA), a well-known signaling phospholipid, is elevated in the cerebrospinal fluid (CSF) and serum of patients with MS compared to non-inflammatory, non-vascular neurological disease patient samples. PIPE-791 is an orally bioavailable, brain penetrant LPA1 small molecule antagonist currently in clinical trials. We have shown previously that PIPE-791 improves clinical scores in the mouse MOG-EAE model of inflammatory demyelination by promoting oligodendrocyte differentiation as well as decreasing microglia activation. In the current study, we build upon these findings and show that the combination of PIPE-791 with submaximal efficacious doses of FTY-720 (fingolimod) ameliorates clinical scores beyond FTY-720 alone. Further, using the cuprizone model of acute demyelination, we observe improvements in remyelination and VEP latency, supporting a direct effect on oligodendrocyte differentiation.

A displacable PET tracer permits real time in vivo characterization of a biological target of interest and provides valuable information on target expression and target engagement by a co-administered competing compound. As such, we identified PIPE-497, an LPA1 antagonist with properties amenable for PET use. For example, in addition to being brain penetrant, PIPE-497 has an LPA1 dissociation  $t_{1/2}$  of only 11.2 minutes, versus PIPE-791 which has a significantly longer  $t_{1/2}$  of 519 minutes. We characterized <sup>3</sup>H-PIPE-497 binding by autoradiography in rodent, non-human primate, and human brain sections, and observed a similar dissociation constant (Kd) across species. Further, consistent with literature LPA1 expression, <sup>3</sup>H-PIPE-497 displays strong specific binding that overlaps with white matter tracts. Binding was also detected in the gray matter, especially in deep layers of cortex, striatum, thalamus, and medulla.

In human brain sections derived from MS patients, <sup>3</sup>H-PIPE-497 distribution coincided with activated microglia in active and mixed active lesions, as determined using <sup>3</sup>H-DPA-713, a marker of the 18-kDa translocator protein (TSPO). Further, <sup>3</sup>H-PIPE-497 binding overlapped with areas enriched with activated microglia and foamy macrophages known to be associated with chronic inflammation and disease severity. These findings encourage the development of PIPE-497 as PET tracer to evaluate MS lesions in clinical development and support targeting LPA1 for treating MS patients with PIPE-791 with advantages not seen with current immunotherapies.

## PIPE-791 IMPROVED DISEASE SCORE IN MOG EAE MODEL

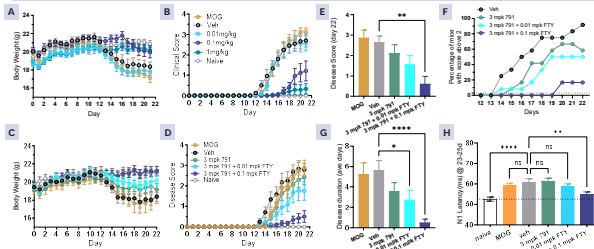


**Figure 1:** Effect of PIPE-791 in combination with FTY720 on MOG EAE disease score and VEPs. The efficacy of different doses of FTY720 was first evaluated on body weight and disease score (A, B) in MOG EAE mouse model. The efficacy of combining PIPE-791 with subthreshold doses of FTY720 were subsequently evaluated on body weight and disease score (C, D). The combination of PIPE-791 (Emglog, ac) with subthreshold doses of FTY720 (0.02, and 0.1 mg/kg, po) improved clinical scores (E, \* $p < 0.001$ , mean  $\pm$  SEM, ANOVA w/ Dunnett's), the number of animal responding to treatment (F, disease duration (G), \* $p < 0.05$ , \*\* $p < 0.0001$ , mean  $\pm$  SEM, ANOVA w/ Dunnett's) and VEP1 latency (H, \* $p < 0.0002$ , \*\* $p < 0.0001$ , mean  $\pm$  SEM, ANOVA w/ Dunnett's). Interestingly, a dose of FTY720 (0.01 mg/kg) that did not improve disease outcome showed efficacy in combination with PIPE-791 on disease duration (G) and VEP1 latency (H).

## EFFECT OF PIPE-791 IN THE CUPRIZONE MODEL FOR DEMYELINATION

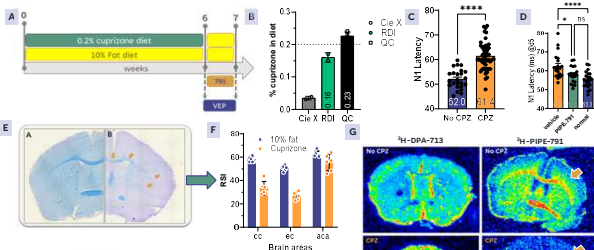


**Figure 2:** PIPE-791 improved visual evoked potential in the cuprizone-induced demyelination model. C57BL/6 female mice were fed an lithium for 4 weeks (A) or a 10% fat diet containing 0.3% of cuprizone (Research Diet Inc (RD)) or a fixed amount of cuprizone spiked into fat diet as measured by LC/MS/MS by Ricardo Solutions (CC) (B). This treatment induced a statistically significant increase in the VEP N1 latency (C) at week 8. Cuprizone was then removed from the diet to initiate remyelination and the cuprizone treated group was dosed with either vehicle or PIPE-791 (3 mg/kg, po) for one week. The N1 latency was decreased for the group treated with PIPE-791 (D, \* $p < 0.0001$ , mean  $\pm$  SEM, ANOVA w/ Dunnett's). A one week post-recovery, the myelin stain Luxol fast blue was still decreased in the corpus callosum (E, F, cc) and external capsule (E, F, ec) but not in the anterior, anterior commissure (E, F, ac) or the internal capsule (not shown) in cuprizone treated mice. Then matched brain coronal sections from mice receiving cuprizone from CC or RD were evaluated for translocator protein (TSPO) and LPA1 binding sites one week after cuprizone recovery (G). Both TSPO (<sup>3</sup>H-DPA-713) and LPA1 (<sup>3</sup>H-PIPE-497) tracers were increased in the corpus callosum and striatum (G). However, the distribution of those tracers appear slightly different suggesting the implication of different cell populations. Further, cellular characterization are under way to determine those. Note the decrease of LPA1 binding sites in the cortex in the cuprizone treated animal (arrow in G).

## REFERENCES

- Xiong D, Ji W, Wu X, Zhou X. Elevated lysophosphatidic acid levels in the serum and cerebrospinal fluid in patients with multiple sclerosis: therapeutic response and clinical implication. *Neuro Res*. 2018;39(4):335-339.
- Wernock KH, Fung K, Housheer DR, Quaresima MM, Burgum MR, Owens GP, Gillett DJ. Proteomic analysis of multiple sclerosis cerebrospinal fluid. *Mol Syst*. 2004 Jun;1(2):135-40.
- Zahrntschke H, Bakos M, Haritoni N, Masabro-Namin SA, Bahmani N, Siroos B. Increased autoantibody activity in multiple sclerosis. *J Neuroimmunol*. 2014 Aug 1;272(1):1-1210-3.
- Feng M, Khoo L, Lohman-Hare, Van den A, Shen, Kellner A, Rankin, Karty, Statnikov, Daniel S, Corbett, Shores A, Sagan, Lan, Liu, Gray, Neuberger, He, Christman, van, Boldingen, Jürgen Weiss, J. Ash Lawrence, Arif J. Green, Stephen J. Fawc, Scott S. Zeman, Jonah R. Chan, 2018. Accelerated remyelination during inflammatory demyelination prevents axonal loss and improves functional recovery. *PLoS One*. 2018;13(12):e0201824.
- van Eden, V. Ransohoff, J. Ransohoff, V. Ransohoff, M. Mason and I. Huitinga. 2018 Progressive multiple sclerosis patients show substantial lesion activity that correlates with clinical disease severity and is a representative autopsy cohort analysis. *Acta Neuropathologica*. 131(4): 511-528.

## <sup>3</sup>H-PIPE-497 AUTORADIOGRAPHY BINDING IN MOUSE BRAIN

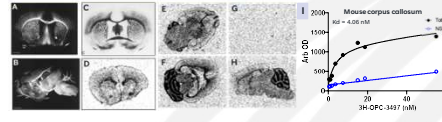


**Figure 3:** <sup>3</sup>H-PIPE-497 ex vivo autoradiography binding in mouse brain. <sup>3</sup>H-PIPE-497 showed strong specific binding in mouse coronal (C) horizontal (D, F) and sagittal (H) brain sections. Non-specific binding (B) was low when an excess of selective cold LPA1 competitor (15  $\mu$ M) was added to the binding incubation mix. The overall brain distribution of <sup>3</sup>H-PIPE-497 was comparable to PLP (A, B, Molloy, 2002) and MBP transgenic mice (C, Gov, 1992). In mouse, <sup>3</sup>H-PIPE-497 Kd is 4.05 nM in the corpus callosum. <sup>3</sup>H-PIPE-497 Kd was 1.42 nM (G). To evaluate the impact of demyelination on <sup>3</sup>H-PIPE-497 binding, Sprague-Dawley rats were injected with 4 $\mu$ l of 1:4.0 LysPC in the corpus callosum (D & E). Animals were sacrificed seven days later and brain sections were incubated with <sup>3</sup>H-PIPE-497 or processed for Sudan Black staining to visualize white matter (D). The contralateral side was used as control for myelin levels (yellow box in D). Both Sudan black staining and <sup>3</sup>H-PIPE-497 binding were reduced by the LysPC injection suggesting a decrease in myelin (D & E). This result suggests that <sup>3</sup>H-PIPE-497 could be used to trace myelin in rat brain and may offer the opportunity to develop PIPE-497 as a PET tracer.

## <sup>3</sup>H-PIPE-497 AUTORADIOGRAPHY BINDING IN RAT BRAIN

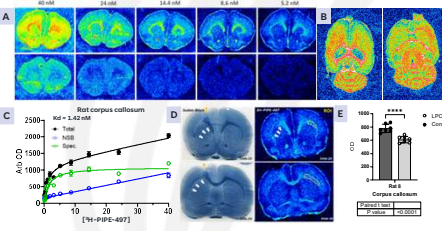


**Figure 4:** <sup>3</sup>H-PIPE-497 ex vivo autoradiography binding in rat brain. <sup>3</sup>H-PIPE-497 showed concentration dependent increase in binding with strong signal to nose in rat brain. The distribution of <sup>3</sup>H-PIPE-497 was particularly strong in white matter in corpus callosum, anterior commissure (A, B, B). In the cerebellum, binding sites overlapped with the molecular layer (B). Binding is also observed in gray matter areas (cortex, striatum, thalamus, pons and medulla) but with lower intensity. In the rat corpus callosum, <sup>3</sup>H-PIPE-497 Kd was 1.42 nM (C). To evaluate the impact of demyelination on <sup>3</sup>H-PIPE-497 binding, Sprague-Dawley rats were injected with 4 $\mu$ l of 1:4.0 LysPC in the corpus callosum (D & E). Animals were sacrificed seven days later and brain sections were incubated with <sup>3</sup>H-PIPE-497 or processed for Sudan Black staining to visualize white matter (D). The contralateral side was used as control for myelin levels (yellow box in D). Both Sudan black staining and <sup>3</sup>H-PIPE-497 binding were reduced by the LysPC injection suggesting a decrease in myelin (D & E). This result suggests that <sup>3</sup>H-PIPE-497 could be used to trace myelin in rat brain and may offer the opportunity to develop PIPE-497 as a PET tracer.

## <sup>3</sup>H-PIPE-497 AUTORADIOGRAPHY BINDING IN NHP BRAIN

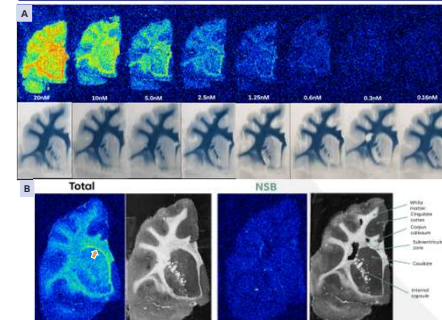


**Figure 5:** <sup>3</sup>H-PIPE-497 ex vivo autoradiography binding in cynomolgus female monkey brain. Like previous findings in mouse and rat, <sup>3</sup>H-PIPE-497 showed a strong specific binding that was concentration dependent and enriched in white matter tracts (A and B). The strongest signal was seen in the subventricular zone (SVZ, arrow in B). Dissociation constant in the corpus callosum, striatum, SVZ and cortex were 4.5, 2.3, 1.7 and 2.9, respectively.

## <sup>3</sup>H-PIPE-497 AUTORADIOGRAPHY BINDING IN HUMAN BRAIN

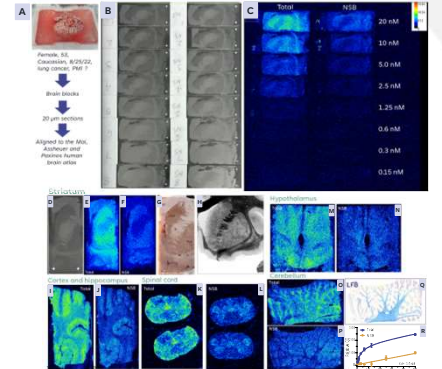


**Figure 6:** <sup>3</sup>H-PIPE-497 ex vivo autoradiography binding in female healthy brain. Upon receiving, whole human brain was dissected into 2-3 cm blocks and frozen on dry ice (A). Striatum sections were generated (B) and incubated with decreasing concentrations of <sup>3</sup>H-PIPE-497 (C). Dissociation constant was determined and found to be 3.5 nM in corpus callosum (E) and 2.8 nM in the putamen (not shown). Binding sites were present in both the white and gray matters with sometime higher intensity in the latter. For example, strong signal was seen in the caudate and putamen as well in the internal capsule (D-H). White matter tracts (corpus callosum, internal and external capsule) are clearly seen in G & H (Mol et al., 2004; Atlas of the human brain) and represent a section of the striatum stained with Sudan black. In the cortex, <sup>3</sup>H-PIPE-497 signal was enriched in the deeper layers and stronger than in the white matter (I-J). NBS: Nonspecific binding, in the sand core (K, L) and hypothalamus (M, N), strong signal could be seen also in gray matter and especially in the medial mammillary nucleus. In the cerebellum, <sup>3</sup>H-PIPE-497 is abundant in the white matter (O, P) as illustrated by myelin staining with Luxol fast blue (Q).

## <sup>3</sup>H-PIPE-497 AUTORADIOGRAPHY BINDING IN MS LESIONS

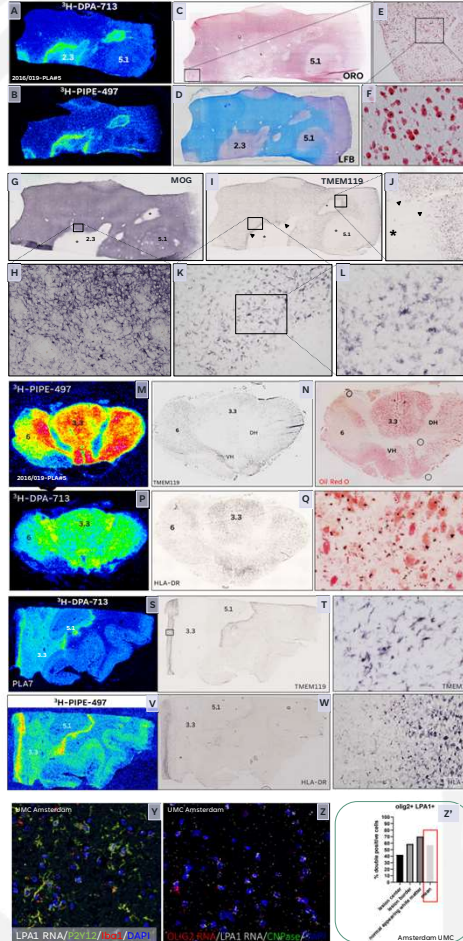


**Figure 7:** <sup>3</sup>H-PIPE-497 and <sup>3</sup>H-DPA-713 ex vivo autoradiography binding with multiple labeling (A-F) and LPA1 receptor cellular gene co-expression with oligodendrocytes and microglia markers (Y-Z) in multiple sclerosis patient brain lesions. Multiple Sclerosis (MS) tissues blocks from three male patients with age ranging from 45-54 years old and with more than 10 years of MS clinical history were obtained from the Netherlands Brain Bank (NBB, Amsterdam). Those tissues blocks from brain areas and spinal cord contained lesions dissected on MRI guidance and were selected to represent a variety of lesions ranging from active, chronic/active and inactive in both the white and gray matters following the classification of MS lesion according to Lucchinetti et al., 2000. For consistency, data from only one patient are illustrated here and showed the binding of TSPO (<sup>3</sup>H-DPA-713, A, P, S) and LPA1 receptor (<sup>3</sup>H-PIPE-497, B, M, V) tracers. Active lesions (score 2-3) in the white matter (A-F) contained numerous foamy cells labeled with Oil Red O (ORO, C, E, F) uniformly distributed in the center of the lesion as well as HLA positive cells (not shown, NBB). The binding of both tracers at the center of the lesion was relatively low, yet higher than the signal observed in the white matter. Another lesion, this time in the gray matter with ramified HLA positive cells with a score 5.1 (NBB) was seen on the lower edge of the lesion that did not contain any cells labeled with ORO or TMEM119, a marker for activated microglia. Interestingly, the border of the lesion displayed a higher binding signal for both tracers that overlapped with the increase in TMEM119 labeling (I-L) probably reflecting an accumulation of activated microglia at the lesion border. We cannot rule out that the accumulation of binding signal could also be due to activated oligodendrocytes, indeed, a slight increase in myelin could be observed in sections labeled with MOG antibody in lesion 2.3 but not 5.1 (G, H). A mixed active/inactive lesion score 3.3 was seen in the thalamic signal core (M-F) with abundant HLA positive (G) and foamy cells (O, R), also displayed very strong binding signal for <sup>3</sup>H-PIPE-497 (M) and a weaker signal for <sup>3</sup>H-DPA-713 (P). A shadow plaque score 6 could also be seen in the lateral column with increased number of activated microglia labeled with TMEM119 (N) and lower level of HLA positive cells and foamy cells displayed a strong binding signal with <sup>3</sup>H-PIPE-497 (M) suggesting that this tracer may label activated microglia as well as foamy macrophages. A subclinical mixed active/inactive lesion score 3.3 as well as a gray matter lesion score 5.1 could be seen with intense staining at the lesion border for <sup>3</sup>H-PIPE-497 (V) and <sup>3</sup>H-DPA-713 (S). A similar distribution pattern could be observed by TMEM119 (T, U) and HLA positive cells (W, X). Cellular expression studies performed in collaboration with the Amsterdam University Medical School revealed abundant expression of LPA1 receptors mRNA detected by Nanostring in Iba0/P2Y12 (Y) and Olig2+2 positive cells (Z). The number of LPA1/Olig2+ cells was found to be increased at the lesions border (Z). LFB= Luxol fast blue.

## CONCLUSION

- PIPE-791 in combination with FTY-720 improves disease scores and VEP N1 latency in MOG EAE mouse model. PIPE-791 also improved VEP N1 latency in the remyelination phase in mouse cuprizone model.
- <sup>3</sup>H-PIPE-497, a selective LPA1 receptor antagonist, displays strong specific binding that overlaps with white matter tracts in all species examined with a Kd ranging from 1.4-4.5nM. Some signal could also be observed in gray matter areas.
- <sup>3</sup>H-PIPE-497 binding in mouse brain follow a similar dynamic range to myelin in ablation or rescuing models.
- In human brain, <sup>3</sup>H-PIPE-497 and <sup>3</sup>H-DPA-713 are particularly prominent in/near activated multiple sclerosis lesions and follow similar labeling patterns suggesting the participation of activated oligodendrocytes, macrophages, microglia and foamy cells.
- These findings encourage the development of PIPE-497 as PET tracer to evaluate MS lesions in clinical development and support targeting LPA1 for treating MS patients with PIPE-791 with advantages not seen with current immunotherapies.